DEMOGRAPHIC RESEARCH
A peer-reviewed, open-access journal of population sciences

DEMOGRAPHIC RESEARCH

VOLUME 54, ARTICLE 40, PAGES 1303–1334
PUBLISHED 17 JUNE 2026
http://www.demographic-research.org/Volumes/Vol54/40/
DOI: 10.4054/DemRes.2026.54.40

Formal Relationship

Fertility timing and the birth squeeze

Robert Schoen

Contents

Demographic Research: Volume 54, Article 40
Formal Relationship

Fertility timing and the birth squeeze

Robert Schoen[1]

Abstract

OBJECTIVE
To provide an in-depth examination of the birth squeeze, the alteration of male and female birth rates by the age-sex composition of the population.

METHODS
Mathematical analyses using reasonable simplifying assumptions are made to find male and female total fertility rates (TFRs), and from them an index of the magnitude of the birth squeeze under exponential, linear, and sinusoidal birth trajectories.

RESULTS
Explicit equations are shown for male and female TFRs and for birth squeeze measures under the three birth trajectories. In all cases, the magnitude of the birth squeeze was approximately proportional to (1) a meaningful measure of population change, (2) the difference between the male and female mean ages of fertility, and (3) the sex ratio at birth. Despite the strong influence of cycle length T in sinusoidal models, the cycle time of the maximum birth squeeze is consistently found near time 30, and the minimum near time $30 + T/2$.

CONTRIBUTION
Birth squeezes are a potentially important, though rarely considered, factor in fertility analyses. Here, easy-to-apply methods are presented that show how male and female fertility rates are affected by population composition, and that measure the magnitude of birth squeezes. New, interpretable regularities are derived that relate birth squeezes to meaningful demographic measures and provide new insights into fertility dynamics.

[1] Department of Sociology, Pennsylvania State University, University Park, PA, USA.
Email: rschoen309@att.net.

1. Introduction

Although it is obvious that human fertility stems from the interaction between males and females, most demographic models and analyses treat fertility in terms of female behavior only. That is unnecessarily constraining, and has led to male behavior being neglected and undervalued. It is increasingly appreciated that male behavior is important, both substantively and theoretically (e.g., Goldscheider, Bernhardt, and Lappegård 2015; Schoen 2010; Vignoli, Drefahl, and DeSantis 2012; Dudel and Klüsener 2021).

Inclusivity with regard to gender issues is all the more important in the contemporary West with the recognition of same-sex unions and the new visibility of non-binary persons. In East and South Asia, striking sex ratio at birth imbalances have arisen with increased access to sex-selective abortion, which directly lead to birth and marriage squeezes (den Boer and Hudson 2017; Guilmoto 2012; Kashyap and Villavicencio 2016). The analysis of Zhang and Li (2020) related a rise in the sex ratio at birth to population aging. The importance of population sex ratios for demographic analysis was recently reinforced by Canudas-Romo, Su, and Hollingshaus (2023), who stress the relevance of these ratios to population policy, individual birth and marriage decisions, and economic behavior.

The fertility behavior of one sex is contingent on the availability of members of the other sex. Appreciating and quantifying that constraint is thus a prerequisite for understanding the behavior that must be described and theoretically explained. Birth squeezes, alterations in male and female fertility rates and levels caused by imbalances in age-sex composition, can potentially have substantial effects on population fertility and population growth (Schoen 1985). Even as the nature of unions changes, birth squeezes remain relevant because births still predominately occur to men and women in relationships.

The related marriage squeeze has received the lion's share of demographic attention, and a substantial literature exists on the subject (Das Gupta 1973; Henry 1972; McFarland 1975; Schoen 1981; Yellin and Samuelson 1977; see the review in Schoen 1988, Part III). The subject is challenging methodologically as it involves the so-called 'two-sex problem' in demography: the fact that one-sex male and female age-specific birth and marriage rates are not sensitive to the available number of persons of the other sex, and thus both male and female rates cannot be held constant when the composition of the population changes.

Although there has been some useful applied work (e.g., Raymo and Park 2020; Uchikoshi, Raymo, and Yoda 2023), there has been little methodological work on the two-sex problem in recent decades (though see Pollak 1990; Iannelli, Martcheva, and Milner 2005). No two-sex approach has been accepted as "the" solution, but it is fair to say that the harmonic mean approach is recognized as "a" solution. We follow that approach as it leads to birth squeeze measures that can be found from one-sex schedules of male and female age-specific rates.

Here, for the first time, the magnitude and patterns of birth squeezes are calculated and examined in the context of populations where births change exponentially, linearly, or cyclically. Using only male and female total fertility rates (TFRs), methods are described for defining and measuring birth squeezes. Two key relationships are presented. The phenomenon is then systematically examined under (1) distinct male and female age-specific fertility schedules, (2) different birth trajectories, and (3) different sex ratios at birth. The contemporary relevance of the birth squeeze is demonstrated using data for Spain 1975–2015, where fertility fell and ages at birth rose. A modest squeeze against women turned into a substantial squeeze against men, distorting the meaning of the female TFR, the standard measure of fertility level.

2. The basic model

We begin by considering what produces birth squeezes. Three factors stand out (Dudel and Klüsener 2021). First, fathers are typically older than mothers, and thus come from different birth cohorts. Second, between cohort differences become important when cohorts are of different size. Third, within-cohort differences emerge when the sex ratio at birth departs from 100 males for every 100 females.

Accordingly, let us construct a model where male birth rates peak at a later age than female birth rates, and the birth trajectory is known. Initially, to reduce complexity, we assume that the sex ratio at birth is 100 males per every 100 females, though how that assumption can be relaxed is considered in Section 5. Throughout, we assume no mortality below age 45, the highest age at reproduction. Reproduction for both sexes begins at age 15. While the highest male age at reproduction could be increased in more complex models, age 45 captures the great majority of male births in contemporary Western populations. For example, in 2012, 95.4% of male births in England and Wales occurred below age 45 (United Kingdom, Office for National Statistics 2013).

The number of births (both male and female) in year t is denoted by $g(t)$. We consider birth trajectories that yield a stable (exponentially growing) population, follow a linear pattern of growth, or describe a zero-growth sine function.

Age-specific birth rates are assumed to vary proportionally over time, thus the ratio of the age 20 to 25 birth rate to the age 15 to 20 birth rate is the same at all time points. That proportionality is a commonly observed pattern (Hobcraft, Menken, and Preston 1982). Such models have been analyzed in Schoen (2024) and in Schoen (2025), where they are termed parastable. The age pattern of fertility is based on the cubic density

function (Schoen 2024)

$$f(x) = \left(-\frac{63}{20} + \frac{\mu}{10}\right) + x\left(\frac{19}{50} - \frac{11\mu}{900}\right) + x^2\left(-\frac{61}{4500} + \frac{\mu}{2250}\right) + x^3\left(\frac{1}{6750} - \frac{\mu}{202500}\right), \tag{1}$$

which ranges over ages 15 to 45, with $\int f(x)\,dx$ equal to 1. Unless otherwise noted, all integrals go from age 15 to age 45. The cubic fertility density of Equation (1) depends only on the mean age of fertility μ, which can vary between ages 27 and 33. That cubic pattern, while not always providing a close fit to observed age-specific fertility rates, does reflect typical age curves of fertility, allows for flexibility in the mean age of fertility, and provides a reasonable basis for analytical work.

Density $f(x)$ can be scaled to any fertility level, preserving the relative size of the age-specific fertility rates. The male or female birth rate age at x and time t, $\varphi(x,t)$ can then be written

$$\varphi_g(x,t) = R_g(t) f_g(x), \tag{2}$$

where $R_g(t)$ is the TFR at time t, and subscript g equals m for males and f for females. In terms of the birth trajectory, the birth rate can be written

$$\varphi_g(x,t) = \frac{g(t) f_g(x)}{\frac{1}{2} g(t-x)} \tag{3}$$

as half the births are male and half female. The male and female TFRs are then

$$R_g(t) = \int \varphi_g(x,t)\,dx = \int \frac{g(t) f_g(x)}{\frac{1}{2} g(t-x)}\,dx. \tag{4}$$

3. Key measures of the birth squeeze

The harmonic mean approach used is based on birth propensities, or two-sex measures of attractiveness (Schoen 1985). Let $J(x,y,t)$ be the propensity for births to males age x and females age y at time t. Then

$$J(x,y,t) = \psi_m(x,y,t) + \psi_f(x,y,t), \tag{5}$$

where $\psi_g(x, y, t)$ is the time t, gender g birth rate for males age x and females age y. The underlying idea is that as the gender composition of the population changes, one age-sex-specific rate goes up while the other goes down, with the sum of those rates remaining constant. The J propensities are thus independent of the age-sex composition of the population.

Significantly for present purposes, it follows that the sum of all the propensities equals the sum of the male and female TFRs, or that

$$\sum\sum J(x, y, t) = \sum [\varphi_m(x, t) + \varphi_f(x, t)] = R_m(t) + R_f(t), \tag{6}$$

where the sums range over all reproductive ages. That total propensity is a two-sex measure of fertility level. Following Schoen (1985), let us define $TFR2(t)$ as the arithmetic mean

$$TFR2(t) = \frac{R_m(t) + R_f(t)}{2}, \tag{7}$$

which provides a two-sex measure of fertility level at time t. As the total number of births is the same for males and females, the difference between $R_m(t)$ and $R_f(t)$ reflects the influence of past population growth and gender differences in mean ages of fertility – in other words, the extent of the birth squeeze. Expressing that difference as a fraction of the two-sex level of fertility yields time t and birth squeeze index U as

$$U(t) = \frac{R_m(t) - R_f(t)}{TFR2(t)}. \tag{8}$$

Thus a theoretically grounded measure of the birth squeeze can be found from the male and female TFRs alone, without the need to know the full array of birth propensities.

Taking a step back, the TFRs themselves can be found from a known birth trajectory. Thus we can use index U to assess the birth squeezes that arise under a variety of birth trajectories, with male and female age-specific birth rate schedules distinguished by different mean ages at birth.

We find two key relationships connecting the birth squeeze to the birth trajectory and to the difference between male and female mean ages of fertility. The first relationship is a close approximation that arises when the birth trajectory is exponential, and is

$$U \approx r\Delta\mu = U_{\text{est}}, \tag{9}$$

where r is the stable (exponential) growth rate, $\Delta\mu$ is the difference between the male mean age of fertility (μ_m), and the female mean age of fertility (μ_f), with that approximation denoted by U_{est}. While the exact equation for U, Equation (A3) in Appendix A, is rather complicated, the simple approximation in Equation (9) is quite accurate. With equal numbers of males and females in every birth cohort, the birth squeeze in a stable population is just the product of the stable rate of growth and the difference between male and female mean ages of fertility. That relationship has not previously been noted.

The second relationship is exact, though a bit less simple. When births increase linearly with slope b and there are 2 births at time 0, the time t birth squeeze index is

$$U(t) = \frac{b\Delta\mu}{2 + b\left[t - \frac{1}{2}(\mu_m + \mu_f)\right]}. \tag{10}$$

The numerator in Equation (10) parallels the relationship in Equation (9). However, the extent of the squeeze varies over time. That change is captured by the denominator, which can be interpreted as the number of births of about a generation earlier. With equal numbers of males and females born, the birth squeeze again reflects the product of a growth rate and the difference between male and female mean ages of fertility. In sinusoidal models, as described below, there is a similar though weaker relationship between U and the amplitude of the sine wave.

We now proceed to derive those key relationships and to describe the birth squeeze in the context of stable, linear, and cyclically stationary populations. We then consider the case where unequal numbers of males and females are born. Finally, we examine the birth squeeze observed in Spain over the years 1975 through 2014.

4. Analyzing birth squeezes in three model populations that have equal numbers of male and female births

Let us now systematically examine the birth squeezes that arise under three birth trajectories: exponential, linear, and sinusoidal. In each case, consistent with the generally observed pattern of fathers being older than mothers, we take the male mean age of fertility to be 33 years, and compare that to patterns with female mean ages of 27 and 30. That gender attribution is imposed, as the cubic density distribution applies to any gender. Following Equation (3), occurrence/exposure age-sex-specific male and female fertility rates are calculated by dividing all births to persons of the specified age by half the population at that age, since there are equal numbers of males and females at every reproductive age.

4.1 Exponential birth trajectory/stable populations

The fixed-rate, stable population birth trajectory is exponential, and scaling the population so that there are two births in reference year t (one male and one female) gives the renewal equation

$$2 = \int e^{-rx} \; R_g(t) \; f_g(x) \; dx, \tag{11}$$

where $R_g(t$ and $f_g(x)$ have distinct male and female values. The exponential growth rate of the stable population is denoted by r. Equation (11) can be solved explicitly for the $R_g(t)$ and U, with the full solutions given in Equations (A2) and (A3), as derived in Appendix A and B.

Table 1 shows TFR and birth squeeze index values for growth rates from -0.04 to $+0.04$. When $r = 0$ there is no birth squeeze. With the male μ fixed at 33, the female μ is set at 30 or 27, so we examine birth squeezes where the male–female mean age difference is either 3 or 6 years.

Table 1: Fertility and birth squeeze measures in stable populations with cubic fertility densities and proportional age change in birth rates

	$\mu_m = 33$		$\mu_f = 27$			$\mu_f = 30$				
r	TFR_m	TFR_f	$TFR2$	U	U_{est}	TFR_f	$TFR2$	U	U_{est}	$\frac{\frac{1}{2}\,[TFR(33) + TFR(27)]}{TFR(30)}$
–0.04	0.519	0.660	0.590	–0.238	–0.240	0.581	0.550	–0.112	–0.120	1.015
–0.03	0.731	0.875	0.803	–0.179	–0.180	0.797	0.764	–0.086	–0.090	1.018
–0.02	1.026	1.157	1.092	–0.120	–0.120	1.088	1.057	–0.058	–0.060	1.003
–0.01	1.435	1.524	1.480	–0.060	–0.060	1.478	1.457	–0.030	–0.030	1.001
0.00	2.000	2.000	2.000	0.000	0.000	2.000	2.000	0.000	0.000	1.000
0.01	2.777	2.615	2.696	0.060	0.060	2.694	2.735	0.030	0.030	1.001
0.02	3.842	3.408	3.625	0.120	0.120	3.612	3.727	0.062	0.060	1.004
0.03	5.295	4.425	4.860	0.179	0.180	4.821	5.058	0.094	0.090	1.008
0.04	7.270	5.726	6.498	0.238	0.240	6.407	6.838	0.126	0.120	1.014

Note: Birth trajectory $g(t) = 2\exp(rt)$.

For all mean ages, the level of fertility varies substantially with the value of r. For $r > 0$, the higher the mean age of fertility, the higher total fertility; for $r < 0$, the opposite is true. The level of fertility varies nearly linearly with the difference between male and female mean ages. As shown in the last column of Table 1,

$$TFR(30) \approx \frac{1}{2}\left[TFR(33) + TFR(27)\right], \tag{12}$$

where $TFR(x)$ is the male or female TFR for mean age of fertility x.

In contrast, birth squeeze index U varies directly and approximately proportionally with r, and U is close to symmetric for r values above and below zero. For example, when $r = \pm .02$, $U = \pm .120$, and when $r = \pm .04$, $U = \pm .240$. Index U values are negative when $r < 0$, indicating a squeeze against males, and are positive when $r > 0$ and there is a birth squeeze against females. For large magnitudes of r and a 6-year difference in mean ages, U values indicate substantial birth squeezes. Even when r has a magnitude of 0.02 and the mean age difference is 3 years, U indicates that the difference between male and female TFRs is 6% of their average.

In Table 1, note that for all values of r, when μ_f is 27 and there is a 6-year gap between male and female mean ages, the value of U is close to twice the value when μ_f is 30 and there is a 3-year difference in mean ages. Second, for all values of r, with $\Delta\mu = (\mu_m - \mu_f)$, we have the approximate first key relationship

$$U \approx r\Delta\mu = U_{\text{est}} \,, \tag{9}$$

a simple relationship despite the complexity of Equation (A3). Under stability, the magnitude of the birth squeeze is well described by that simple product of two factors: the stable growth rate and the difference between mean male and mean female ages of fertility. As fertility is constant in a stable population, that value of U is independent of time.

4.2 Populations with linear growth

With the birth density of Equation (1), let the linear birth trajectory be given by

$$g(t) = 2 + bt, \tag{13}$$

defined only for positive values of $g(t)$. Using Equation (13) in a renewal equation analogous to Equation (11), we can evaluate the integral and find

$$R(t) = \frac{2 + bt}{2 + b(t - \mu)} = \frac{g(t)}{g(t - \mu)}. \tag{14}$$

Equations (13) and (14) show the simple relationships that link births and fertility levels in linear parastable models.

Using Equation (8), the linear birth squeeze index gives the second key relationship

$$U(t) = \frac{b(\mu_m - \mu_f)}{2 + b\left[t - \frac{1}{2}(\mu_m + \mu_f)\right]}. \tag{10}$$

In the linear case, $U(t)$ has a numerator equal to the slope times $\Delta\mu$, but with a denominator of $g\left(t - \frac{1}{2}[\mu_m + \mu_f]\right)$. With that average of two mean ages, the denominator is approximately the number of births a generation earlier. When slope $b > 0$, $U(t)$ approaches zero as t increases to infinity.

Table 2 shows values of TFRs and $U(t)$ for male mean age 33 and female mean ages 27 and 30. At time 40, slopes are shown for values between -0.04 and $+0.04$, and at time 80 for slopes between -0.02 and $+0.04$ (to avoid negative values of g). For a given slope b, values of U are generally smaller in magnitude than for comparable values of r in Table 1, and smaller in magnitude when $b > 0$ than when $b < 0$. The birth squeeze index varies monotonically with slope b, and declines over time when $b > 0$. At both times 40 and 80, the value of U when the difference in mean ages of fertility is 6 is about twice the value of U when the difference in means is 3.

Table 2: Fertility and birth squeeze measures under linear growth in births with cubic fertility densities and proportional age change in birth rates

Linear slope (*b*)	$\mu_m = 33$ *TFR*$_m$	*TFR*$_f$	$\mu_f = 27$ *TFR*2	*U*	*TFR*$_f$	$\mu_f = 30$ *TFR*2	*U*
			t = 40				
–0.04	0.465	0.541	0.503	–0.150	0.500	0.483	–0.072
–0.03	0.894	0.994	0.944	–0.106	0.941	0.918	–0.052
–0.02	1.290	1.379	1.335	–0.067	1.333	1.312	–0.033
–0.01	1.658	1.711	1.685	–0.032	1.684	1.671	–0.016
0.00	2.000	2.000	2.000	0.000	2.000	2.000	0.000
0.01	2.319	2.254	2.286	0.029	2.286	2.302	0.014
0.02	2.617	2.476	2.547	0.055	2.545	2.581	0.028
0.03	2.896	2.678	2.787	0.078	2.783	2.839	0.040
0.04	3.158	2.857	3.008	0.100	3.000	3.079	0.051
			t = 80				
–0.02	0.755	0.851	0.803	–0.120	0.800	0.777	–0.058
–0.01	1.569	1.633	1.601	–0.040	1.600	1.584	–0.020
0.00	2.000	2.000	2.000	0.000	2.000	2.000	0.000
0.01	2.267	2.213	2.240	0.024	2.240	2.254	0.012
0.02	2.449	2.353	2.401	0.040	2.400	2.424	0.020
0.03	2.581	2.451	2.516	0.051	2.514	2.547	0.026
0.04	2.680	2.524	2.602	0.060	2.600	2.640	0.030

Note: Birth trajectory $g(t) = 2 + bt$. For $t = 80$, $g(t)$ is not defined for slope values of -0.03 and -0.04.

4.3 Cyclically stationary populations

Cyclically stationary populations extend the basic life table stationary population model, and can provide useful models for dynamic demographic analyses. Here, the initial operationalization sets base birth level $a = 2$, amplitude $b = 0.2$ or 0.3, and focuses on cycle lengths T of 40, 60, and 80 years.

Let the birth trajectory be $g(t) = 2 + b\ \sin(\omega t)$, where frequency $\omega = \frac{2\pi}{T}$. Then the renewal equation can be explicitly integrated. Appendices C and D derive and show the resultant TFRs and values of birth squeeze index U in Equations (C4) and (C7).

Table 3 shows fertility and birth squeeze measures when births vary sinusoidally, $\mu_m = 33$, and $\mu_f = 27$ or 30. Panel A shows values when $T = 40$ years and $b = 0.3$, and Panel B when $T = 40$ years but $b = 0.2$. Consistent with Equation (C7), U values are directly proportional to $\Delta\mu = \mu_m - \mu_f$, and approximately proportional to amplitude b. Keeping $b = 0.3$, Panel C shows values when $T = 60$ years and Panel D when $T = 80$ years.

Table 3: Fertility and birth squeeze measures under sinusoidal growth in births with cubic fertility densities and proportional age change in birth rates

	$\mu_m = 33$	$\mu_f = 27$			$\mu_f = 30$		
Cycle point (t)	TFR_m	TFR_f	$TFR2$	U	TFR_f	$TFR2$	U
A. Cycle length $T = 40$ years; amplitude $b = 0.3$							
5	2.028	2.159	2.093	–0.062	2.091	2.060	–0.031
10	2.198	2.413	2.305	–0.093	2.300	2.249	–0.046
15	2.268	2.433	2.351	–0.070	2.348	2.308	–0.034
20	2.178	2.178	2.178	0.000	2.178	2.178	0.000
25	1.966	1.833	1.900	0.070	1.897	1.932	0.036
30	1.783	1.624	1.704	0.093	1.700	1.742	0.048
35	1.745	1.639	1.692	0.062	1.690	1.717	0.032
40	1.849	1.849	1.849	0.000	1.849	1.849	0.000
B. Cycle length $T = 40$ years; amplitude $b = 0.2$							
5	2.019	2.107	2.063	–0.042	2.062	2.041	–0.021
10	2.134	2.271	2.202	–0.062	2.200	2.167	–0.031
15	2.177	2.279	2.228	–0.046	2.227	2.202	–0.023
20	2.115	2.115	2.115	0.000	2.115	2.115	0.000
25	1.978	1.890	1.934	0.046	1.933	1.956	0.023
30	1.858	1.746	1.802	0.062	1.800	1.829	0.032
35	1.828	1.753	1.791	0.042	1.790	1.809	0.021
40	1.897	1.897	1.897	0.000	1.897	1.897	0.000

Table 3: (Continued)

Cycle point (t)	$\mu_m = 33$ TFR_m	TFR_f	$\mu_f = 27$ $TFR2$	U	TFR_f	$\mu_f = 30$ $TFR2$	U
C. Cycle length $T = 60$ years; amplitude $b = 0.3$							
5	2.203	2.368	2.285	–0.072	2.283	2.243	–0.036
10	2.459	2.569	2.514	–0.044	2.512	2.486	–0.022
15	2.602	2.602	2.602	0.000	2.602	2.602	0.000
20	2.569	2.459	2.514	0.044	2.512	2.541	0.022
25	2.368	2.203	2.285	0.072	2.283	2.325	0.037
30	2.082	1.924	2.003	0.079	2.000	2.041	0.040
35	1.807	1.694	1.750	0.064	1.748	1.778	0.033
40	1.610	1.553	1.582	0.036	1.581	1.596	0.018
45	1.523	1.523	1.523	0.000	1.523	1.523	0.000
50	1.553	1.610	1.582	–0.036	1.581	1.567	–0.018
55	1.694	1.807	1.750	–0.064	1.748	1.721	–0.032
60	1.924	2.082	2.003	–0.079	2.000	1.962	–0.039
D. Cycle length $T = 80$ years; amplitude $b = 0.3$							
5	2.371	2.438	2.404	–0.028	2.404	2.387	–0.014
10	2.543	2.543	2.543	0.000	2.543	2.543	0.000
15	2.625	2.553	2.589	0.028	2.589	2.607	0.014
20	2.598	2.472	2.535	0.050	2.533	2.566	0.025
25	2.473	2.234	2.399	0.062	2.397	2.435	0.032
30	2.285	2.144	2.214	0.064	2.212	2.249	0.032
35	2.073	1.959	2.016	0.056	2.014	2.044	0.029
40	1.870	1.794	1.832	0.041	1.831	1.851	0.021
45	1.701	1.665	1.683	0.022	1.683	1.692	0.011
50	1.582	1.582	1.582	0.000	1.582	1.582	0.000
55	1.521	1.555	1.538	–0.022	1.538	1.530	–0.011
60	1.525	1.590	1.557	–0.041	1.557	1.541	–0.020
65	1.596	1.689	1.642	–0.056	1.641	1.619	–0.028
70	1.732	1.847	1.790	–0.064	1.788	1.760	–0.031
75	1.924	2.048	1.986	–0.062	1.984	1.954	–0.031
80	2.149	2.259	2.204	–0.050	2.203	2.176	–0.025

Note: Birth trajectory $g(t) = 2 + b \sin(\omega t)$.

In all four panels, $U(t)$ fluctuates fairly symmetrically about zero. The approximate proportionality of $U(t)$ to the product $b\Delta\mu$ holds here as well. Notably, so does the approximate linearity of the TFR, at all cycle lengths and cycle points, across different mean ages of fertility – that is, $\frac{1}{2}\left[TFR(\mu = 27) + TFR(\mu = 33)\right] \approx TFR(\mu = 30)$.

The magnitude of the birth squeeze varies greatly with cycle length. Table 4, with values derived as described in Appendix E, shows that with $b = 0.3$ and $\Delta\mu = 6$, extreme values of U range from ± 0.035 when $T = 20$ to ± 0.097 when $T = 40$. As T increases beyond 40 years, the magnitude of U diminishes. There appears to be an effect from the ratio of cycle length T to 30 years, the length of the reproductive age span. A larger T also implies smaller up and down slopes in the sine curve. In the sinusoidal models considered, birth squeezes are mild to moderate in magnitude, and may well be

relevant to substantive analyses of fertility. The timing of extreme U values can be closely approximated by two simple relationships. The maximum U occurs around cycle point $t = 30$ (equivalent to $t = 10$ when $T = 20$). The minimum U occurs near $t = 30 + \frac{T}{2}$.

Table 4: Maximum and minimum cycle points and values of birth squeeze index U for sinusoidal birth trajectories, male mean age of fertility (μ_m) of 33 and female mean age of fertility (μ_f) of 27

Cycle length (T)		20	40	60	80
A. Cycle year (t)	Maximum U	10.0	29.5	28.9	28.3
	Minimum U	20.0	10.5	61.1	71.7
B. Birth squeeze (U)	Maximum	0.0351	0.0968	0.0793	0.0645
	Minimum	–0.0351	–0.0968	–0.0793	–0.0645

Note: Birth trajectory $g(t) = 2 + 0.3\sin(\omega t)$.

Table 5, calculated as described in Appendix F, shows that a somewhat similar pattern holds for the timing and level of extreme values of the male and female TFRs. For most cycle lengths, the time of the maximum TFR is approximated by cycle point $t = 15$, and the minimum TFR by $t = 15 + \frac{T}{2}$. Cycle length $T = 70$ shows the largest maximum TFR (2.609) and the smallest minimum TFR (1.522), indicating a swing in the level of fertility of 1.1 children around a central value of 2. However, values when $T < 40$ often do not fit that pattern.

Table 5: Maximum and minimum cycle points and values of total fertility rate $R(t)$ with sinusoidal birth trajectories, mean age of fertility 30, and cycle lengths (T) from 20 to 100 years

Cycle length (T)	Cycle point	Maximum TFR	Minimum cycle point	TFR
20	5	2.290	15	1.707
30	7.5	2.200	22.5	1.781
35	11.570	2.238	28.354	1.755
40	13.630	2.356	32.716	1.670
50	14.821	2.534	39.221	1.560
60	15	2.602	45	1.523
70	14.899	2.609	50.573	1.522
80	14.694	2.589	56.052	1.536
90	14.445	2.557	61.475	1.557
100	14.179	2.523	66.861	1.579

Note: Birth trajectory $g(t) = 2 + 0.3\sin(\omega t)$.

Figure 1 depicts the relationships between birth trajectory $g(t)$ and the male and female TFRs when cycle length T is 40, 60, and 80 years and $\mu_f = 27$. For all three cycle lengths, the TFRs are approximately sinusoidal and generally show more variability than the birth trajectory. Because $\mu_m > \mu_f$, the peak of R_f always precedes that of R_m, as can be appreciated by switching the male and female $f(x)$ schedules.

Figure 1: Birth trajectory $g(t)$ and male and female total fertility rates in cyclically stationary populations with cycle length (T) of 40, 60, and 80 years

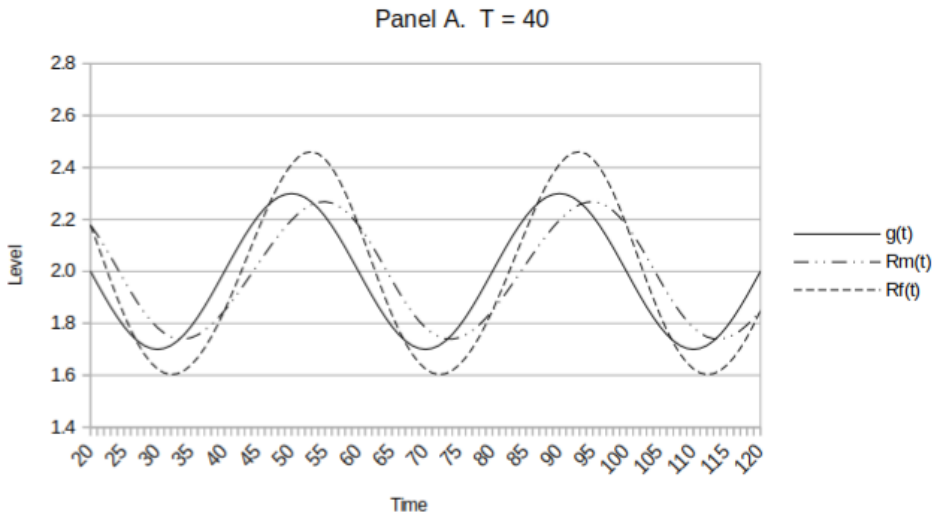

Figure 1: (Continued)

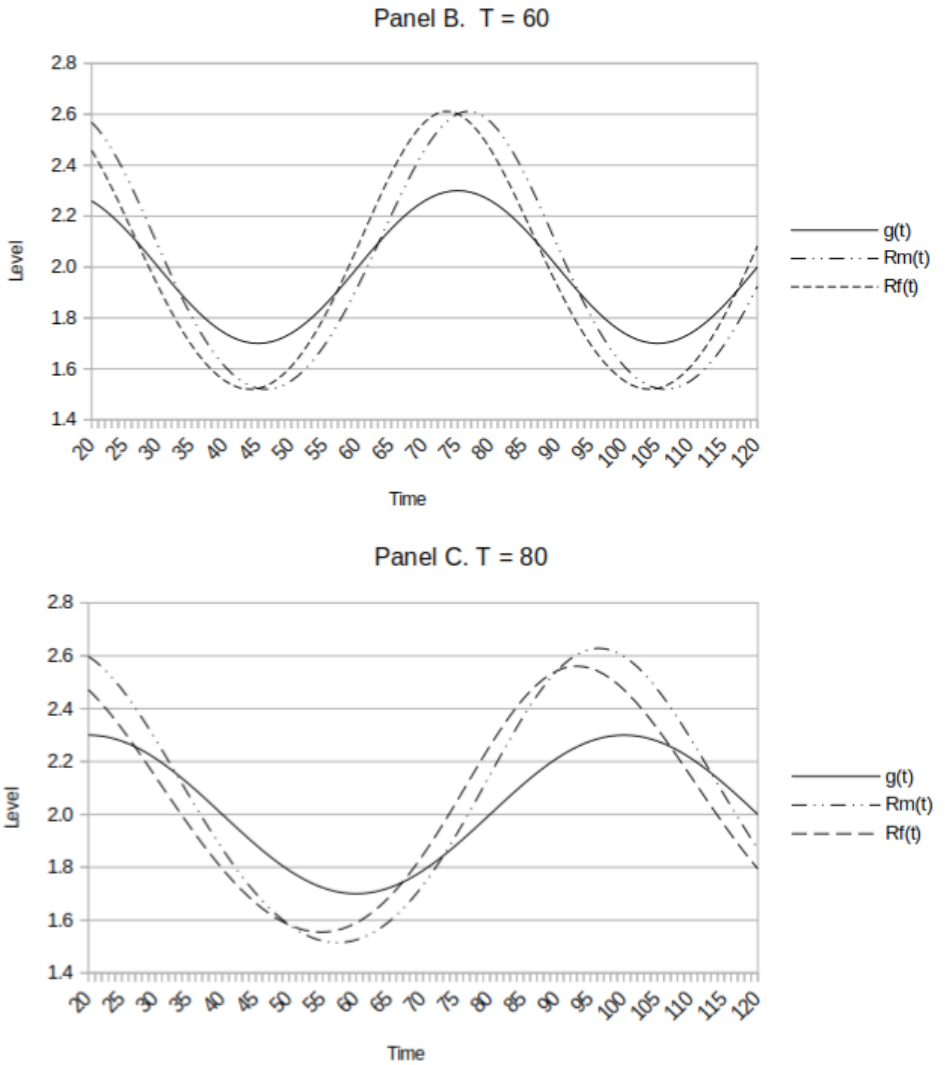

Figure 2 shows how g, $TFR2$, and U vary within cycles for cycle lengths 40, 60, and 80 and $\mu_f = 27$. The value of $U(t)$ is multiplied by a factor of 25 to achieve a common vertical scale. At all three cycle lengths, $TFR2$ is close to g and approximately sinusoidal. The trajectory of the birth squeeze index is also rather sinusoidal, but values above and

below zero are a bit skewed. The order of the peaks when $T = 40$ is g before $TFR2$, with the peak of U at roughly the trough of g and $TFR2$. When $T = 60$, it is U following the common maximum of g and $TFR2$, and when $T = 80$, it is $TFR2$ before g, which is before U.

Figure 2: Birth trajectory $g(t)$, two-sex total fertility rate $TFR2$, and birth squeeze index U in cyclically stationary populations with cycle length (T) of 40, 60, and 80 years

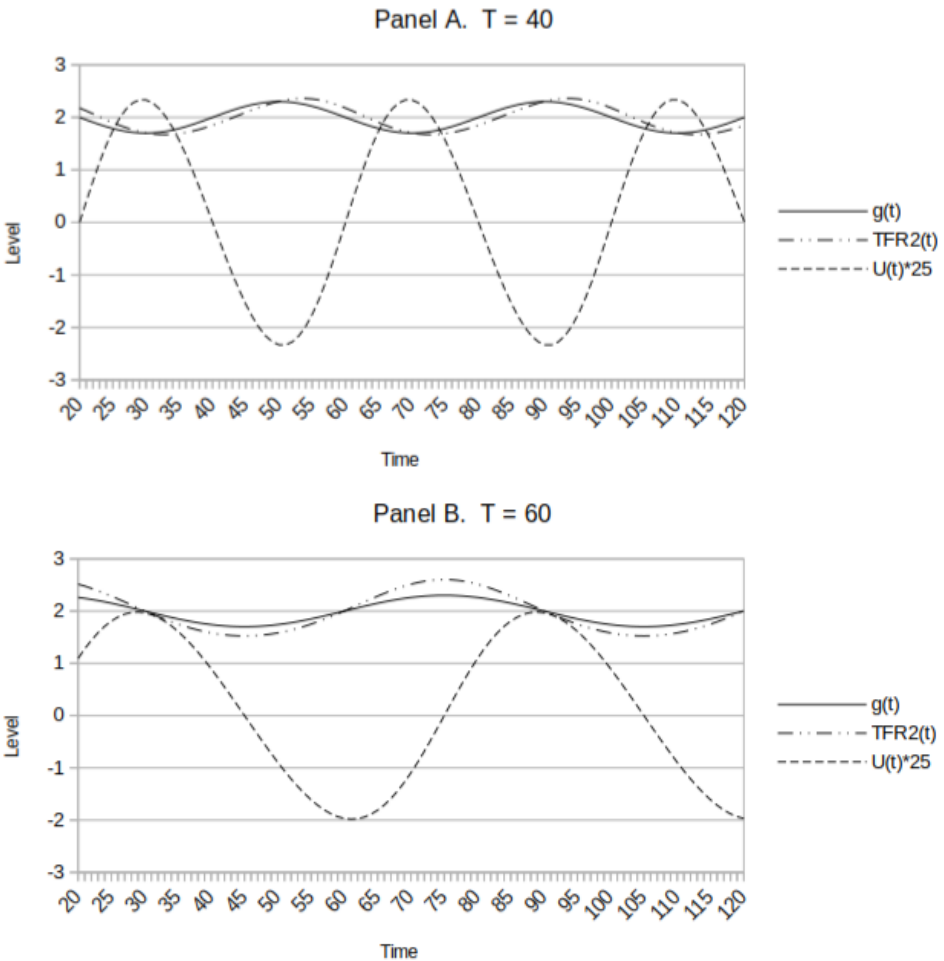

Figure 2: (Continued)

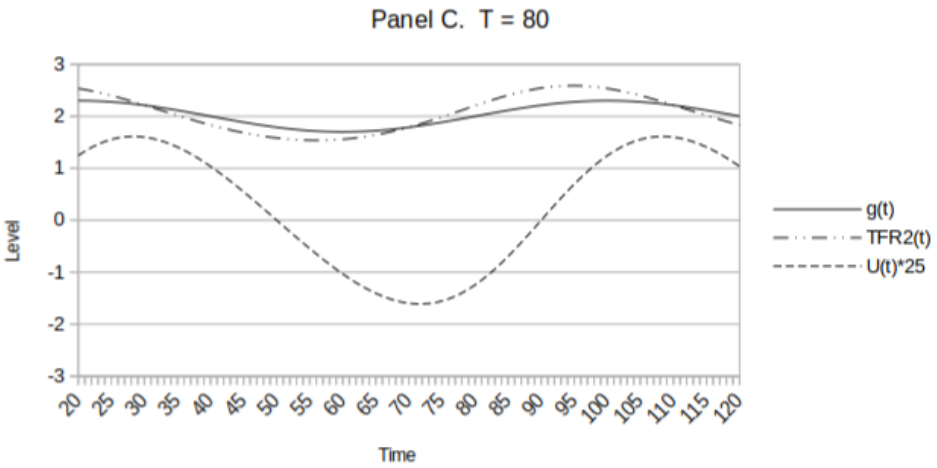

In sum, when births are sinusoidal, birth squeeze index U varies proportionally with the difference between male and female mean birth ages and approximately proportionally with sine amplitude b. In those ways, the behavior of U parallels Equation (9). However, the magnitude of $U(t)$varies with cycle length T. At all cycle lengths, the maximum value of $U(t)$ occurs at about cycle point 30, and the minimum at about $t = 30 + \frac{T}{2}$.

5. Examining birth squeezes in the case of unequal sex ratios at birth

To this point, we have assumed that equal numbers of males and females are born. In most populations, however, there are about 105 males born for every 100 females, or a male proportion of 0.512. Moreover, some contemporaneous populations, notably in East and South Asia, have experienced considerable numbers of sex-selective abortions, and have had substantially larger sex ratios at birth. In South Korea in 1990, there were 116 males born for every 100 females, and in Vietnam in 2009, four provinces had over 120 male births for every 100 female births (den Boer and Hudson 2017).

Now let the male proportion be denoted by s. Using our cubic fertility densities and with fertility rates changing proportionally at all ages, we can examine the effect on U when $s \neq 0.5$. Appendix G derives the birth squeeze index for any value of s, and finds

$$U_s(t) = 2\frac{R_m(t)(1-s) - sR_f(t)}{R_m(t)(1-s) + sR_f(t)} \tag{15}$$

for adjusted birth squeeze index $U_s(t)$. Equation (15) shows that the sex ratio effect on the birth squeeze depends not only on male proportion s, but also on the male and female TFRs. An example can be informative. Let $R_m = 1.4$ and $R_f = 1.6$, with Equation (8) then giving $U = -0.133$. However, with $s = 0.53$, Equation (15) yields an adjusted $U_s = -0.252$, a birth squeeze against males that is nearly twice as great.

In short, the relationships developed in the previous sections can readily be modified to reflect unequal sex ratios at birth. Values of s that depart from one-half can magnify birth squeezes.

6. Birth squeezes in contemporary Spain

Male age-specific fertility rates are now available for a number of populations. Dudel and Klüsener (2021) examine them for 17 high-income countries, and those values are included in the Human Fertility Collection of the Human Fertility Database. The findings of Dudel and Klüsener (2021) reinforce the idea that male–female fertility differences are largely driven by differences in mean age at birth and differential cohort size.

Spain is a particularly illustrative case, as in recent decades it has experienced both a substantial decline in fertility and a major swing in birth squeeze index U. Table 6 presents fertility data for Spain 1975–2014, including index U. Spanish fertility fell from a TFR_f of 2.765 in 1975 to 1.154 in 1995, before increasing to about 1.3. The mean age at birth increased by about 3 years for both men and women, with the age difference staying about 3 years. In 1985 there was a modest birth squeeze of 0.039 against women, but by 2010 there was a substantial birth squeeze of -0.091 against men. In 2010, with a TFR_f of 1.37, the TFR_m was 1.25, some 0.12 children less. That is a nontrivial difference. The female TFR, despite being very low, overstates the population's fertility propensity, as measured by the $TFR2$. The birth squeeze is not just a phenomenon of high fertility traditional populations, but it can also characterize contemporary low fertility, high-income populations as well.

Table 6: Male and female total fertility rates and birth squeeze measures, Spain, 1975–2014

	Total fertility rates				Birth squeeze	Mean ages at birth		
Year	TFR_m	TFR_f	TFR_2	TFR_m–TFR_f	Index U	μ_m	μ_f	$\mu_m - \mu_f$
1975	2.855	2.765	2.810	0.090	0.032	31.72	28.66	3.06
1980	2.291	2.216	2.254	0.070	0.033	31.06	28.21	2.85
1985	1.706	1.640	1.673	0.066	0.039	31.42	28.46	2.96
1990	1.401	1.361	1.381	0.040	0.029	31.82	28.86	2.96
1995	1.172	1.154	1.163	0.018	0.015	32.85	29.99	2.86
2000	1.195	1.207	1.201	–0.012	–0.010	33.66	30.75	2.91
2005	1.252	1.329	1.290	–0.077	–0.060	33.91	30.91	3.00
2010	1.250	1.369	1.310	–0.119	–0.091	34.30	31.20	3.10
2014	1.211	1.320	1.266	–0.109	–0.086	34.63	31.78	2.87

Source: Data from the Human Fertility Collection in the Human Fertility Database.

7. Summary and conclusions

The birth squeeze reflects the dependence of male and female age-specific fertility rates on the number of males and females in the population. To a greater or lesser degree, a birth squeeze is always present in human populations, suggesting that both male and female birth rates merit consideration in fertility analyses. Here, the magnitude of the birth squeeze effect, and its determinants, are explored in depth using the harmonic mean approach to the two-sex problem. In that context, the birth squeeze can be accurately measured from data on male and female total fertility rates alone. Making the reasonable assumptions that fertility rates vary proportionately over age from a cubic base pattern, we show, for the first time, how the effects of (1) different birth trajectories, (2) differences in male and female mean ages of fertility, and (3) sex ratios at birth affect the magnitude of a squeeze. Exponential, linear, and cyclical birth trajectories are examined, assuming no mortality below age 45, the highest age of reproduction. Substantial similarities in the nature of birth squeeze effects characterize all three birth trajectories.

Under the exponential birth trajectory of a stable population, with equal numbers of male and female births, birth squeeze index U is closely approximated by two simple factors: (1) the rate of population growth and (2) the difference between male and female mean ages of fertility ($\Delta\mu$). A similar pattern arises with linear birth trajectories, where U is approximately equal to the linear slope times $\Delta\mu$, divided by the number of births a generation earlier.

Cyclically stationary models are given particular attention as they recognize fertility fluctuations and can be a useful platform for long- and short-term population analyses. In such sinusoidal models, relationships are more complicated, but an explicit solution for index U is presented in Equation (C7). Although the effects of cycle length T are sub-

stantial, U remains proportional to $\Delta\mu$ and approximately proportional to the amplitude of the sine wave. Remarkably, within each cycle, the birth squeeze consistently attains its maximum value near cycle year 30, and its minimum value near cycle year $30 + \frac{T}{2}$.

When there are deviations from equal numbers of male and female births, the birth squeeze can be found using the relatively simple adjustment provided in Equation (15). Given the high sex ratios at birth in a number of East and South Asian countries, fertility analyses of those nations need to explicitly recognize their short- and long-term implications.

The present study focuses on models, not data, but the experience of Spain between 1975 and 2014 demonstrates the relevance of the birth squeeze to the analysis of contemporary populations. Over those 40 years, fertility dropped some 40% to very low levels, while a modest birth squeeze against women turned into a substantial birth squeeze against men. Birth squeezes are as relevant to low fertility populations as to high fertility populations.

In a world where all persons can no longer be divided into two genders, and where there are marked differences in preferences within the male and female genders, consideration of compositional 'squeezes' is an appropriate extension to customary fertility and marriage analyses. The approach advanced here to measuring the extent of such effects is a contribution to that goal. Male and female ages at birth matter, as they have relevance for child health, mortality, and migration (cf Dudel and Klüsener 2021).

As always, models are simplifications, and their results are influenced by the assumptions used. Alternative assumptions are worthy of examination. Furthermore, little attention has been paid to birth squeezes following short to midterm birth fluctuations. The birth spike following the 1967 abortion change in Romania is an extreme example (cf Bradatan 2009), but less dramatic changes appear common and merit examination.

Noteworthy two-sex population interaction effects frequently exist and deserve more attention in demographic analyses, as do fertility rates by age of father. The present analysis of the birth squeeze has revealed that the extent of such effects on birth rates can readily be gauged and related to meaningful demographic variables, and has provided new insights into contemporary fertility dynamics.

References

Beyer, W.H. (1978). *CRC standard mathematical tables*. (25th Ed). West Palm Beach, FL: CRC Press.

Bradatan, C.E. (2009). Large but adaptable? A successful population policy and its long term effects. *Population Research and Policy Review* 28: 389–404. doi:10.1007/s11113-008-9104-7.

Canudas-Romo, V., Su, W., and Hollingshaus, M. (2023). Variable-r in sex ratios: Formulas in honor of Jim Vaupel. *Demographic Research* 49(26): 693–722. doi:10.4054/DemRes.2023.49.26.

Das Gupta, P. (1973). Growth of U.S. population, 1940–1971, in the light of an interactive two-sex model. *Demography* 10(4): 543–565. doi:10.2307/2060882.

den Boer, A. and Hudson, V.M. (2017). Patrilineality, son preference, and sex selection in South Korea and Vietnam. *Population and Development Review* 43(1): 119–147. doi:10.1111/padr.12041.

Dudel, C. and Klüsener, S. (2021). Male-female fertility differentials across 17 high-income countries: Insights from a new data resource. *European Journal of Population* 37: 417–441. doi:10.1007/s10680-020-09575-9.

Goldscheider, F.K., Bernhardt, E., and Lappegård, T. (2015). The gender revolution: A framework for understanding changing family and demographic behavior. *Population and Development Review* 41(2): 207–239. doi:10.1111/j.1728-4457.2015.00045.x.

Guilmoto, C.Z. (2012). Skewed sex ratios at birth and future marriage squeeze in China and India, 2005–2100. *Demography* 49(1): 77–100. doi:10.1007/s13524-011-0083-7.

Henry, L. (1972). Nuptiality. *Theoretical Population Biology* 3(2): 135–152. doi:10.1016/0040-5809(72)90023-8.

Hobcraft, J., Menken, J., and Preston, S. (1982). Age, period and cohort effects in demography: A review. *Population Index* 48(1): 4–43. doi:10.2307/2736356.

Iannelli, M., Martcheva, M., and Milner, F.A. (2005). *Gender-structured population modeling: Mathematical methods, numerics, and simulations*. Frontiers in Applied Mathematics. Philadelphia, PA: Society for Industrial and Applied Mathematics. doi:10.1137/1.9780898717488.

Kashyap, R. and Villavicencio, F. (2016). The dynamics of son preference, technology diffusion, and fertility decline underlying distorted sex ratios at birth: A simulation approach. *Demography* 53(5): 1261–1281. doi:10.1007/s13524-016-0500-z.

McFarland, D.D. (1975). Models of marriage formation and fertility. *Social Forces* 54(1): 66–83. doi:10.1093/sf/54.1.66.

Office for National Statistics (2013). Birth in England and Wales: 2012. Newport, United Kingdom: Office for National Statistics. Table downloaded 8/6/2024 from https://www.ons.gov.uk/peoplepopulationandcommunity/birthsdeathsandmarriages/livebirths/bulletins/birthsummarytablesenglandandwales/2013-07-10.

Pollak, R. (1990). Two-sex demographic models. *Journal of Political Economy* 98(2): 399–420. doi:10.1086/261683.

Raymo, J.M. and Park, H. (2020). Marriage decline in Korea: Changing composition of the domestic marriage market and growth in international marriage. *Demography* 57(1): 171–194. doi:10.1007/s13524-019-00844-9.

Schoen, R. (1981). The harmonic mean as the basis of a realistic two-sex marriage model. *Demography* 18(2): 201–216. doi:10.2307/2061093.

Schoen, R. (1985). Population growth and the birth squeeze. *Social Science Research* 14(3): 251–265. doi:10.1016/0049-089X(85)90004-3.

Schoen, R. (1988). *Modeling multigroup populations*. New York: Plenum Press. doi:10.1007/978-1-4899-2055-3.

Schoen, R. (2010). Gender competition and family change. *Genus* 66: 95–120.

Schoen, R. (2024). Fertility quantum and tempo with cubic age-specific birth rates. *Demographic Research* 51(42): 1351–1370. doi:10.4054/DemRes.2024.51.42.

Schoen, R. (2025). Exponential age-change in fertility, proportional age-change, and stability. In: Schoen, R. (ed.). *Advances in social demography*. Cham: Springer: 407–431. doi:10.1007/978-3-031-89737-5_17.

Uchikoshi, F., Raymo, J.M., and Yoda, S. (2023). Family norms and declining first marriage rates: The role of sibship position in the Japanese marriage market. *Demography* 60(3): 939–963. doi:10.1215/00703370-10741873.

Vignoli, D., Drefahl, S., and DeSantis, G. (2012). Whose job instability affects the likelihood of becoming a parent in Italy? A tale of two partners. *Demographic Research* 26(2): 41–62. doi:10.4054/DemRes.2012.26.2.

Yellin, J. and Samuelson, P.A. (1977). Comparison of linear and nonlinear models for human population dynamics. *Theoretical Population Biology* 11(1): 105–126. doi:10.1016/0040-5809(77)90010-7.

Zhang, Z. and Li, Q. (2020). Population aging caused by a rise in the sex ratio at birth. *Demographic Research* 43(32): 969–992. doi:10.4054/DemRes.2020.43.32.

Appendix A: Derivation of birth squeeze index U when the birth trajectory is exponential

The derivation here is based on the model in Section 2 with the cubic fertility density of Equation (1). The exponential renewal equation is shown in Equation (11), and birth squeeze index U is defined in Equation (8).

Using Equation (11), the int function, as shown in the Maple program in Appendix B, yields the result

$$R_g(t) = \frac{67500\, r^4 e^{15r}}{e^{-30r} Y_g(r,\mu) + Z_g(r,\mu)}$$

with

$$Y_g(r,\mu) = 75r^2(\mu_g - 27) + 15r(\mu_g - 29) + (\mu_g - 30)$$

and

$$Z_g(r,\mu) = 75r^2(33 - \mu_g) + 15r(\mu_g - 31) + (30 - \mu_g). \tag{A1}$$

When $\mu_g = 30$, Equation (A1) reduces to

$$R_g(t) = \frac{4500\, r^3 e^{15r}}{e^{-30r}(15r+1) + (15r-1)}. \tag{A2}$$

The birth squeeze index is then

$$U = \frac{2(\mu_m - \mu_f)\left[(75r^2 - 15r + 1) - e^{-30r}(75r^2 + 15r + 1)\right]}{e^{-30r} F_1 + F_2}$$

where

$$F_1 = (\mu_m + \mu_f)(75r^2 + 15r + 1) - 30(135r^2 + 29r + 2)$$

and

$$F_2 = (\mu_m + \mu_f)(-75r^2 + 15r - 1) + 30(165r^2 - 31r + 2). \tag{A3}$$

If males and females have the same mean age of fertility, $U = 0$.

Appendix B: Maple program to calculate birth squeeze measures in stable populations

Figure A-1: Code for Maple program to calculate birth squeeze measures in stable populations

```
> #   Program BSQ ExpoUeqs
> restart;
> with (linalg):
Warning, new definition for norm
Warning, new definition for trace
> #     To calculate BSQ values in stable populations
> gt:=2*exp(r*t);
```

$$gt := 2\,e^{(r\,t)}$$

```
> #    With proportional age-change and cubic base density
> #  R(t) = 2 / [int {exp(-rx) f(x) dx}.  To integrate the
  denominator
>
> IntRinv:=int( exp(-r*x)*( -63/20. +mu/10 +x*(19/50 -11*mu/900)
  +x*x*(-61/4500 +mu/2250) + x*x*x*(1/6750 -mu/202500)), x=15..45);
```

$$IntRinv := .00002962962963\,(-2025.\,e^{(-45.\,r)}\,r^2 + 75.\,e^{(-45.\,r)}\,\mu\,r^2 - 435.\,e^{(-45.\,r)}\,r + 15.\,e^{(-45.\,r)}\,\mu\,r - 30.\,e^{(-45.\,r)} + e^{(-45.\,r)}\,\mu + 2475.\,e^{(-15.\,r)}\,r^2 - 75.\,e^{(-15.\,r)}\,\mu\,r^2 - 465.\,e^{(-15.\,r)}\,r + 15.\,e^{(-15.\,r)}\,\mu\,r + 30.\,e^{(-15.\,r)} - 1.\,e^{(-15.\,r)}\,\mu)\,/\,r^4$$

```
> #   To calculate the Total Fertility Rates
> TFRm:=2*33750*(r^4)*exp(15*r) / ( exp(-30*r)*(75*r^2*(mu1-27)
  +15*r*(mu1-29) +mu1-30) + 75*r^2*(33-mu1) +15*r*(mu1-31) +
  30-mu1);
```

$$TFRm := 67500\,r^4\,e^{(15\,r)}\,/\,(e^{(-30\,r)}\,(75\,r^2\,(\mu1-27)+15\,r\,(\mu1-29)+\mu1-30)+75\,r^2\,(33-\mu1)+15\,r\,(\mu1-31)+30-\mu1)$$

```
> TFRf:=2*33750*(r^4)*exp(15*r) / ( exp(-30*r)*(75*r^2*(mu2-27)
  +15*r*(mu2-29) +mu2-30) + 75*r^2*(33-mu2) +15*r*(mu2-31) +
  30-mu2);
```

$$TFRf := 67500\,r^4\,e^{(15\,r)}\,/\,(e^{(-30\,r)}\,(75\,r^2\,(\mu2-27)+15\,r\,(\mu2-29)+\mu2-30)+75\,r^2\,(33-\mu2)+15\,r\,(\mu2-31)+30-\mu2)$$

```
> TFR2:=.5*(TFRm+TFRf);
```

$$TFR2 := 33750.0\,r^4\,e^{(15\,r)}\,/\,(e^{(-30\,r)}\,(75\,r^2\,(\mu1-27)+15\,r\,(\mu1-29)+\mu1-30)+75\,r^2\,(33-\mu1)+15\,r\,(\mu1-31)+30-\mu1) + 33750.0\,r^4\,e^{(15\,r)}\,/\,(e^{(-30\,r)}\,(75\,r^2\,(\mu2-27)+15\,r\,(\mu2-29)+\mu2-30)+75\,r^2\,(33-\mu2)+15\,r\,(\mu2-31)+30-\mu2)$$

```
> #  To find birth squeeze index U
> U:=(TFRm-TFRf)/TFR2:
> simplify(%);
```

Page 1

Figure A-1: (Continued)

$$
\begin{aligned}
&-2.\,e^{(30.\,r)}\,(75.\,e^{(-30.\,r)}\,r^2\,\mu2 - 2025.\,e^{(-30.\,r)}\,r^2 + 15.\,e^{(-30.\,r)}\,r\,\mu2 - 435.\,e^{(-30.\,r)}\,r + e^{(-30.\,r)}\,\mu2\\
&\quad - 30.\,e^{(-30.\,r)} + 2475.\,r^2 - 75.\,r^2\,\mu2 + 15.\,r\,\mu2 - 465.\,r + 30. - 1.\,\mu2)\,(75.\,e^{(-30.\,r)}\,r^2\,\mu1\\
&\quad - 2025.\,e^{(-30.\,r)}\,r^2 + 15.\,e^{(-30.\,r)}\,r\,\mu1 - 435.\,e^{(-30.\,r)}\,r + e^{(-30.\,r)}\,\mu1 - 30.\,e^{(-30.\,r)} + 2475.\,r^2\\
&\quad - 75.\,r^2\,\mu1 + 15.\,r\,\mu1 - 465.\,r + 30. - 1.\,\mu1)\,(-75.\,r^2\,\mu2 - 15.\,r\,\mu2 - 1.\,\mu2 + 75.\,r^2\,\mu2\,e^{(30.\,r)}\\
&\quad - 15.\,r\,\mu2\,e^{(30.\,r)} + \mu2\,e^{(30.\,r)} + 75.\,r^2\,\mu1 + 15.\,r\,\mu1 + \mu1 - 75.\,r^2\,\mu1\,e^{(30.\,r)} + 15.\,r\,\mu1\,e^{(30.\,r)}\\
&\quad - 1.\,\mu1\,e^{(30.\,r)})\,/\,((75.\,e^{(-30.\,r)}\,r^2\,\mu2 - 4050.\,e^{(-30.\,r)}\,r^2 + 15.\,e^{(-30.\,r)}\,r\,\mu2 - 870.\,e^{(-30.\,r)}\,r\\
&\quad + e^{(-30.\,r)}\,\mu2 - 60.\,e^{(-30.\,r)} + 4950.\,r^2 - 75.\,r^2\,\mu2 + 15.\,r\,\mu2 - 930.\,r + 60. - 1.\,\mu2\\
&\quad + 75.\,e^{(-30.\,r)}\,r^2\,\mu1 + 15.\,e^{(-30.\,r)}\,r\,\mu1 + e^{(-30.\,r)}\,\mu1 - 75.\,r^2\,\mu1 + 15.\,r\,\mu1 - 1.\,\mu1)\,(-75.\,r^2\,\mu2\\
&\quad + 2025.\,r^2 - 15.\,r\,\mu2 + 435.\,r - 1.\,\mu2 + 30. - 2475.\,r^2\,e^{(30.\,r)} + 75.\,r^2\,\mu2\,e^{(30.\,r)} - 15.\,r\,\mu2\,e^{(30.\,r)}\\
&\quad + 465.\,r\,e^{(30.\,r)} - 30.\,e^{(30.\,r)} + \mu2\,e^{(30.\,r)})\,(-75.\,r^2\,\mu1 + 2025.\,r^2 - 15.\,r\,\mu1 + 435.\,r - 1.\,\mu1 + 30.\\
&\quad - 2475.\,r^2\,e^{(30.\,r)} + 75.\,r^2\,\mu1\,e^{(30.\,r)} - 15.\,r\,\mu1\,e^{(30.\,r)} + 465.\,r\,e^{(30.\,r)} - 30.\,e^{(30.\,r)} + \mu1\,e^{(30.\,r)}))
\end{aligned}
$$

```
> EstU:=r*(mu1-mu2);
```

$$EstU := r\,(\mu1 - \mu2)$$

```
>
```

Source: Programmed by Robert Schoen.

Appendix C: Derivation of the total fertility rate and birth squeeze index when the birth trajectory is sinusoidal

The derivation here is based on the model in Section 2. It is applicable to both male and female TFRs, using the appropriate mean age of fertility (μ).

With the birth trajectory given by

$$g(t) = 2 + b\sin(\omega t)\,, \tag{C1}$$

the renewal equation can be written as

$$g(t) = \int \frac{1}{2} g(t-x)R(t)f(x)dx\,, \tag{C2}$$

where the integral ranges over reproductive ages 15 to 45 and $f(x)$ is the cubic density function of Equation (1). Rearranging Equation (C2) gives

$$R(t) = \frac{g(t)}{\int \frac{1}{2} g(t-x)f(x)dx}. \tag{C3}$$

To solve for $R(t)$, we integrate $DD(t)$, the integral expression in the denominator of Equation (C3) and use that value to calculate the TFR. As shown in Appendix D, the int function in Maple yields

$$R_g(t) = \frac{2 + b\sin(\omega t)}{1 + (\frac{b}{67500\omega^4})(Y(t) + V(t))}, \tag{C4}$$

where $Y(t) = 30\omega(\mu_g - 30)\cos[\omega(t-30)]\cos(15\omega) + 30\omega\sin[\omega(t-30)]\sin(15\omega)$ and $V(t) = 2(30-\mu_g)(1-75\omega^2)\cos[\omega(t-30)]\sin(15\omega) - 450\omega^2\sin[\omega(t-30)]\cos(15\omega)$. Equation (C4) makes use of the trigonometric identities (Beyer 1978: 168)

$$\begin{aligned} \sin\alpha + \sin\beta &= 2\sin\left(\frac{\alpha+\beta}{2}\right)\cos\left(\frac{\alpha-\beta}{2}\right), \qquad \sin(-\alpha) = -\sin\alpha \\ \cos\alpha + \cos\beta &= 2\cos\left(\frac{\alpha+\beta}{2}\right)\cos\left(\frac{\alpha-\beta}{2}\right), \qquad \cos(-\alpha) = \cos\alpha\,. \end{aligned} \tag{C5}$$

Equation (C4) simplifies considerably when $\mu_g = 30$. In that case,

$$R_g(t) = \frac{2 + b\sin(\omega t)}{1 + b\sin[\omega(t-30)]F}$$

with

$$F = \frac{\sin(15\omega) - 15\omega\cos(15\omega)}{2250\omega^3}. \tag{C6}$$

For the birth squeeze index of Equation (8), Appendix D provides an expression for U which, using Equation (C5), can be rearranged and rewritten to yield

$$U(t) = \frac{2b(\mu_m - \mu_f)X(t)}{67500\omega^4 - b(\mu_m + \mu_f)X(t) - 30b\,(W(t) + Z(t))},$$

where

$$\begin{aligned} X(t) &= \cos[\omega(t-30)]\left[(1-75\omega^2)\sin(15\omega) - 15\omega\cos(15\omega)\right] \\ W(t) &= \omega\cos[\omega(t-30)] + 15\omega^2\sin[\omega(t-15)] \end{aligned}$$

and

$$Z(t) = \cos[\omega(t-30)]\left[29\omega\cos(15\omega) + 135\omega^2\sin(15\omega) - 2\sin(15\omega)\right]. \tag{C7}$$

Expressions X, W, and Z are functions of w and t alone, and are independent of amplitude b and the male and female mean ages of fertility.

Appendix D: Maple program to calculate birth squeeze measures in sinusoidal populations

Figure A-2: Code for Maple program to calculate birth squeeze measures in sinusoidal populations

```
> #  Program BSQ SineUeqs
> restart;
> with (linalg):
Warning, new definition for norm
Warning, new definition for trace
> #     To calculate BSQ measures when g(t) is sinusoidal
> #   Each calculation is specific to T, b, and cycle point t
> #   Male and female values are shown for TFRs and MACs
> #   The male mu is always 33; the female either 27 or 30
> #    For all T, frequency w = 2pi/T.  srb = 100:100
> #T:=60;
> #w:=2*3.14159265/T;
> #    To integrate f(x)g(t-x) with cubic f(x), for males
> #mu:=33; b:=.3; t:=60; muf:=27;
>
> #   To integrate .5*g(t-x)f(x) over the reproductive ages to find
  DDmint and then TFR = g(t)/DDmint
> DDmint:=.5*(-1/33750)*(-2025*b*w^2*sin(-45*w+w*t)-b*mu*sin(-45*w+w
  *t)+435*b*cos(-45*w+w*t)*w-67500*w^4+75*b*mu*sin(-45*w+w*t)*w^2-15
  *b*mu*cos(-45*w+w*t)*w+30*b*sin(-45*w+w*t)+465*b*cos(-15*w+w*t)*w+
  2475*b*w^2*sin(-15*w+w*t)+b*mu*sin(-15*w+w*t)-75*b*mu*sin(-15*w+w*
  t)*w^2-15*b*mu*cos(-15*w+w*t)*w-30*b*sin(-15*w+w*t))/(w^4);
```

$$DDmint := -.00001481481482\,(-2025\,b\,w^2\sin(-45\,w+w\,t)-b\,\mu\sin(-45\,w+w\,t)+435\,b\cos(-45\,w+w\,t)\,w-67500\,w^4+75\,b\,\mu\sin(-45\,w+w\,t)\,w^2-15\,b\,\mu\cos(-45\,w+w\,t)\,w+30\,b\sin(-45\,w+w\,t)+465\,b\cos(-15\,w+w\,t)\,w+2475\,b\,w^2\sin(-15\,w+w\,t)+b\,\mu\sin(-15\,w+w\,t)-75\,b\,\mu\sin(-15\,w+w\,t)\,w^2-15\,b\,\mu\cos(-15\,w+w\,t)\,w-30\,b\sin(-15\,w+w\,t))\Big/w^4$$

```
> Rm:=(2+b*sin(w*t))/DDmint:
> simplify(%);
```

$$.00002000000000\,w^4\,(.6750000000\,10^{10}+.3374999999\,10^{10}\,b\sin(w\,t))\Big/(2025.\,b\,w^2\sin(-45.\,w+w\,t)+b\,\mu\sin(-45.\,w+w\,t)-435.\,b\cos(-45.\,w+w\,t)\,w+67500.\,w^4-75.\,b\,\mu\sin(-45.\,w+w\,t)\,w^2+15.\,b\,\mu\cos(-45.\,w+w\,t)\,w-30.\,b\sin(-45.\,w+w\,t)-465.\,b\cos(-15.\,w+w\,t)\,w-2475.\,b\,w^2\sin(-15.\,w+w\,t)-1.\,b\,\mu\sin(-15.\,w+w\,t)+75.\,b\,\mu\sin(-15.\,w+w\,t)\,w^2+15.\,b\,\mu\cos(-15.\,w+w\,t)\,w+30.\,b\sin(-15.\,w+w\,t))$$

```
>
> Y:=30*w*(muf-30)*cos(w*(t-30))*cos(15*w) +
  30*w*sin(w*(t-30))*sin(15*w);
```

$$Y := 30\,w\,(muf-30)\cos(w\,(t-30))\cos(15\,w)+30\,w\sin(w\,(t-30))\sin(15\,w)$$

```
> V:= 2*(30-muf)*(1-75*w^2)*cos(w*(t-30))*sin(15*w) -
  450*(w^2)*sin(w*(t-30))*cos(15*w);
```

Page 1

Figure A-2: (Continued)

$$V := 2\,(30 - muf)\,(1 - 75\,w^2)\cos(w\,(t-30))\sin(15\,w) - 450\,w^2\sin(w\,(t-30))\cos(15\,w)$$

```
> Rf:=(2+b*sin(w*t)) / (  1 + (b/(67500*w^4))*(Y+V) ):
> simplify(%);
```

$$33750\,((2 + b\sin(w\,t))\,w^4) \Big/ (33750\,w^4 + 15\,b\,w\cos(w\,(t-30))\cos(15\,w)\,muf$$
$$- 450\,b\,w\cos(w\,(t-30))\cos(15\,w) + 15\,b\,w\sin(w\,(t-30))\sin(15\,w)$$
$$+ 30\,b\cos(w\,(t-30))\sin(15\,w) - 2250\,b\cos(w\,(t-30))\sin(15\,w)\,w^2$$
$$- b\cos(w\,(t-30))\sin(15\,w)\,muf + 75\,b\cos(w\,(t-30))\sin(15\,w)\,muf\,w^2$$
$$- 225\,b\,w^2\sin(w\,(t-30))\cos(15\,w))$$

```
>
> #       To calculate index U
> X:=cos(w*(t-30))*( (1-75*w^2)*sin(15*w) - 15*w*cos(15*w) );
```

$$X := \cos(w\,(t-30))\,((1 - 75\,w^2)\sin(15\,w) - 15\,w\cos(15\,w))$$

```
> W:=w*cos(w*(t-15)) + 15*(w^2)*sin(w*(t-15));
```

$$W := w\cos(w\,(t-15)) + 15\,w^2\sin(w\,(t-15))$$

```
> Z:=cos(w*(t-30))*( 29*w*cos(15*w) + 135*(w^2)*sin(15*w) -
  2*sin(15*w) );
```

$$Z := \cos(w\,(t-30))\,(29\,w\cos(15\,w) + 135\,w^2\sin(15\,w) - 2\sin(15\,w))$$

```
> U:=2*(Rm-Rf)/(Rm+Rf):
> simplify(%);
```

$$-2.\,(33750.\,w^4 - .5062500000\,10^{11}\,b\,w\cos(w\,(t-30.))\cos(15.\,w)\,muf$$
$$+ .1518750000\,10^{13}\,b\,w\cos(w\,(t-30.))\cos(15.\,w)$$
$$- .5062500000\,10^{11}\,b\,w\sin(w\,(t-30.))\sin(15.\,w)$$
$$- .1012500000\,10^{12}\,b\cos(w\,(t-30.))\sin(15.\,w)$$
$$+ .7593750000\,10^{13}\,b\cos(w\,(t-30.))\sin(15.\,w)\,w^2$$
$$+ .3374999999\,10^{10}\,b\cos(w\,(t-30.))\sin(15.\,w)\,muf$$
$$- .2531249999\,10^{12}\,b\cos(w\,(t-30.))\sin(15.\,w)\,muf\,w^2$$
$$+ .7593750000\,10^{12}\,b\,w^2\sin(w\,(t-30.))\cos(15.\,w) + .3417187500\,10^{13}\,b\,w^2\sin(-45.\,w + w\,t)$$
$$+ .1687500000\,10^{10}\,b\,\mu\sin(-45.\,w + w\,t) - .7340625000\,10^{12}\,b\cos(-45.\,w + w\,t)\,w$$
$$- .1265625000\,10^{12}\,b\,\mu\sin(-45.\,w + w\,t)\,w^2 + .2531250000\,10^{11}\,b\,\mu\cos(-45.\,w + w\,t)\,w$$
$$- .5062500000\,10^{11}\,b\sin(-45.\,w + w\,t) - .7846875000\,10^{12}\,b\cos(-15.\,w + w\,t)\,w$$
$$- .4176562500\,10^{13}\,b\,w^2\sin(-15.\,w + w\,t) - .1687500000\,10^{10}\,b\,\mu\sin(-15.\,w + w\,t)$$
$$+ .1265625000\,10^{12}\,b\,\mu\sin(-15.\,w + w\,t)\,w^2 + .2531250000\,10^{11}\,b\,\mu\cos(-15.\,w + w\,t)\,w$$
$$+ .5062500000\,10^{11}\,b\sin(-15.\,w + w\,t)) \Big/ (.2278125000\,10^{15}\,w^4$$
$$+ .5062499999\,10^{11}\,b\,w\cos(w\,(t-30.))\cos(15.\,w)\,muf$$
$$- .1518750000\,10^{13}\,b\,w\cos(w\,(t-30.))\cos(15.\,w)$$

Page 2

Figure A-2: (Continued)

$$
\begin{aligned}
&+ .5062499999\ 10^{11}\ b\ w \sin(w\ (t-30.))\ \sin(15.\ w)\\
&+ .1012500000\ 10^{12}\ b \cos(w\ (t-30.))\ \sin(15.\ w)\\
&- .7593749998\ 10^{13}\ b \cos(w\ (t-30.))\ \sin(15.\ w)\ w^2\\
&- .3374999999\ 10^{10}\ b \cos(w\ (t-30.))\ \sin(15.\ w)\ muf\\
&+ .2531249999\ 10^{12}\ b \cos(w\ (t-30.))\ \sin(15.\ w)\ muf\ w^2\\
&- .7593749998\ 10^{12}\ b\ w^2 \sin(w\ (t-30.))\ \cos(15.\ w) + .3417187500\ 10^{13}\ b\ w^2 \sin(-45.\ w + w\ t)\\
&+ .1687500000\ 10^{10}\ b\ \mu \sin(-45.\ w + w\ t) - .7340625000\ 10^{12}\ b \cos(-45.\ w + w\ t)\ w\\
&- .1265625000\ 10^{12}\ b\ \mu \sin(-45.\ w + w\ t)\ w^2 + .2531250000\ 10^{11}\ b\ \mu \cos(-45.\ w + w\ t)\ w\\
&- .5062500000\ 10^{11}\ b \sin(-45.\ w + w\ t) - .7846875000\ 10^{12}\ b \cos(-15.\ w + w\ t)\ w\\
&- .4176562500\ 10^{13}\ b\ w^2 \sin(-15.\ w + w\ t) - .1687500000\ 10^{10}\ b\ \mu \sin(-15.\ w + w\ t)\\
&+ .1265625000\ 10^{12}\ b\ \mu \sin(-15.\ w + w\ t)\ w^2 + .2531250000\ 10^{11}\ b\ \mu \cos(-15.\ w + w\ t)\ w\\
&+ .5062500000\ 10^{11}\ b \sin(-15.\ w + w\ t))
\end{aligned}
$$

[>

Source: Programmed by Robert Schoen.

Appendix E: Finding extreme values of birth squeeze index U when the birth trajectory is sinusoidal

When the sinusoidal birth trajectory is given by

$$g(t) = 2 + b\sin(\omega t)\ , \tag{E1}$$

the birth squeeze index is the complicated expression in Equation (C7). The usual method for finding extreme values is to take the derivative with respect to time, set that derivative equal to zero, and find the values of t that satisfy that equation. Here, attempts to apply that usual method were not successful.

Instead, extreme values were found by employing functional iteration on Equation (C7), with calculations done in Maple. Cycle lengths of 20, 40, 60, and 80 years were examined, with $\mu_m = 33$, $\mu_f = 27$, and $b = 0.3$. Iteration on t continued until the maximum and minimum values of $U(t)$ were found, with time measured to the nearest tenth of a year.

Appendix F: Finding extreme values of the total fertility rate when the birth trajectory is sinusoidal

When the sinusoidal birth trajectory is given by

$$g(t) = 2 + b\sin(\omega t)\ , \tag{F1}$$

the TFR is the complicated expression in Equation (C4). However, setting the mean age of fertility (μ) equal to 30 years yields the simpler expression in Equation (C6). With $b = 0.3$, Equation (C6) was examined for cycle lengths from 20 to 100.

Following the customary approach to extreme values, Maple was used to differentiate Equation (C6) with respect to time, and that derivative was set equal to zero. The result was a complicated quadratic equation. When numerically solved by Maple, it yielded the times of the maximum and minimum TFR values, which led to finding the extreme TFR values.

Appendix G: Finding birth squeeze index U when s is the male proportion of births

For males, the general renewal equation can be written

$$g(t) = \int RS_m(t) f_m(x) s\, g(t-x) dx\ , \tag{G1}$$

where RS denotes the TFR when s is the proportion of births that are male. With $g(t)$ considered independent of s, it follows that

$$\frac{g(t)}{\int f_m(x) g(t-x) dx} = sRS_m(t) = \frac{1}{2} R_m(t) \tag{G2}$$

and that the male TFR adjusted for the sex ratio at birth is

$$RS_m(t) = \frac{R_m(t)}{2s}\ . \tag{G3}$$

Following the same procedure, the female adjusted TFR is

$$RS_f(t) = \frac{R_f(t)}{2(1-s)} \,. \tag{G4}$$

Thus if $s > \frac{1}{2}$, $\quad RS_m < R_m \quad$ and $\quad RS_f > R_f$.

Straightforward algebra in Equations (G3) and (G4) then yields

$$TFR2S(t) = \frac{R_m(t)(1-s) + sR_f(t)}{4s(1-s)} \tag{G5}$$

for the adjusted $TFR2$ and, from Equation (G5)

$$U_s(t) = 2\frac{R_m(t)(1-s) - sR_f(t)}{R_m(t)(1-s) + sR_f(t)} \tag{G6}$$

for the adjusted birth squeeze index.